

Supporting Information

For

Scavenger-supported photocatalytic evidence of an extended type I electronic structure of $\text{TiO}_2@\text{Fe}_2\text{O}_3$ interface

*Anita Trenczek-Zajac^{*1}, Milena Synowiec^{*1}, Katarzyna Zakrzewska², Karolina Zazakowny¹, Kazimierz Kowalski³, Andrzej Dziedzic⁴ and Marta Radecka¹*

¹Faculty of Materials Science and Ceramics, AGH University of Science and Technology,
Krakow, Poland,

²Faculty of Computer Science, Electronics and Telecommunications, AGH University of
Science and Technology, Krakow, Poland

³Faculty of Metals Engineering and Industrial Computer Science, AGH University of Science
and Technology, Krakow, Poland

⁴Institute of Physics, College of Natural Sciences, University of Rzeszow, Rzeszow, Poland

***Corresponding author:**

milsyn@agh.edu.pl, anita.trenczek-zajac@agh.edu.pl

KEYWORDS

TiO₂, Fe₂O₃, heterostructures, band diagram, interface, electron transfer, photocatalysis

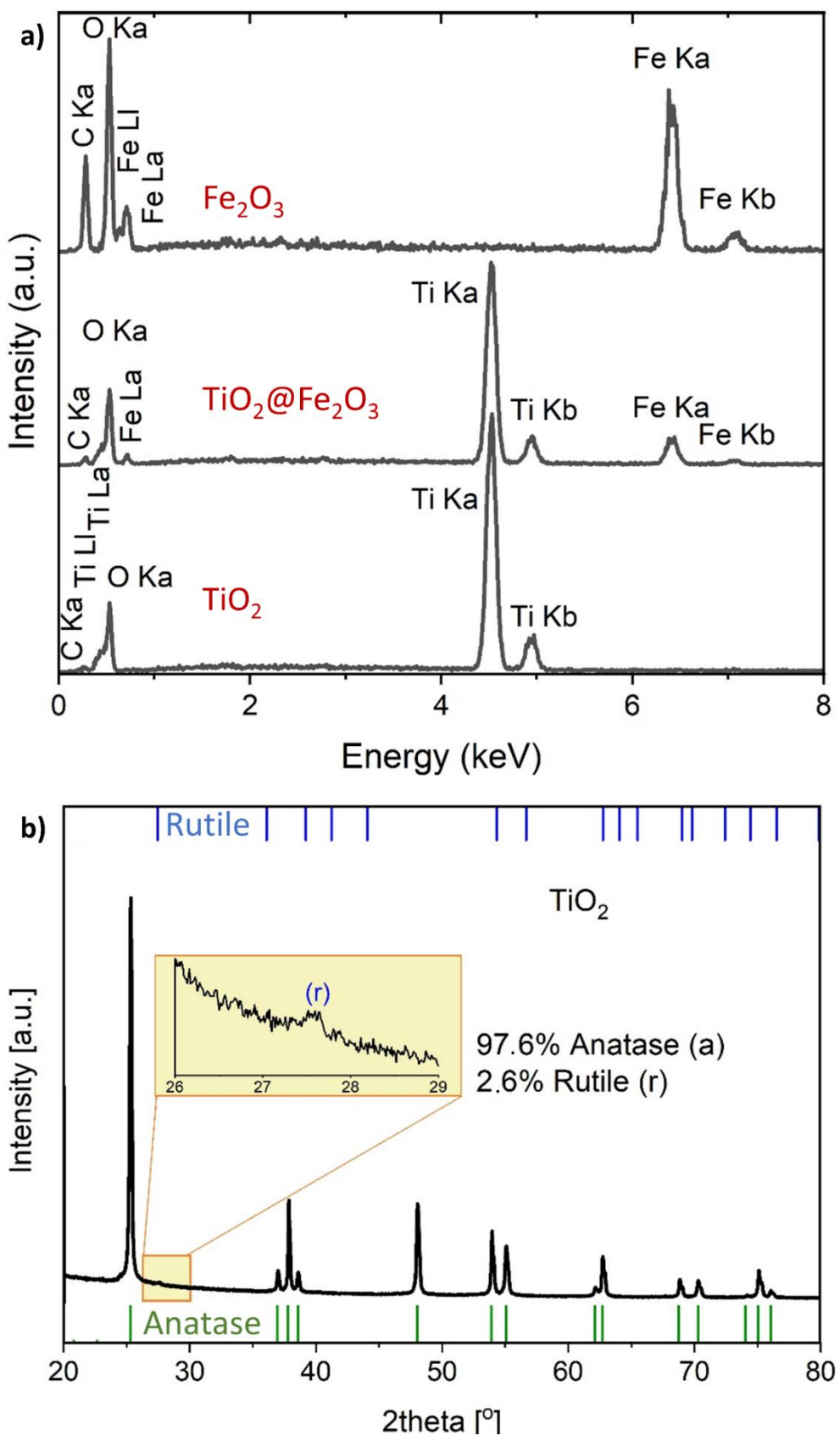


Figure S1. a) EDX spectrum of selected nanomaterials, b) X-ray diffraction pattern of TiO_2 nanocrystals with traces of rutile.

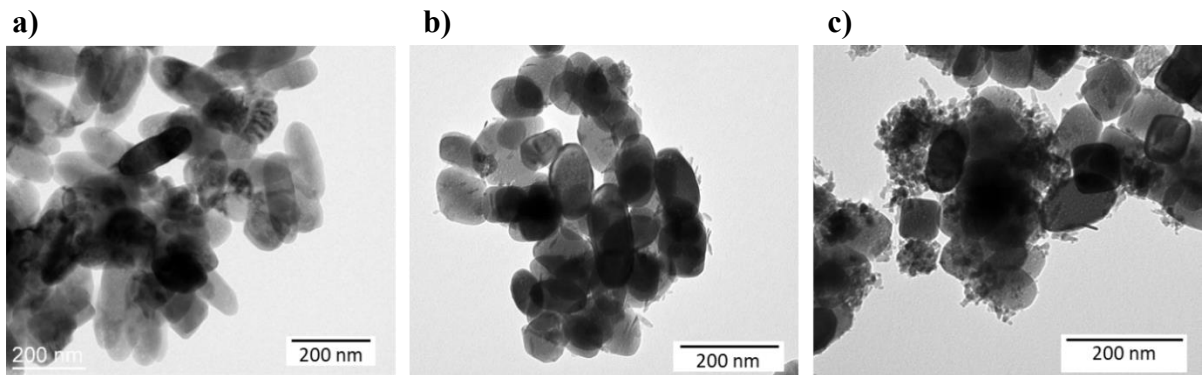


Figure S2. TEM images of a) $\text{TiO}_2@2\%\text{Fe}_2\text{O}_3$, b) $\text{TiO}_2@10\%\text{Fe}_2\text{O}_3$, c) $\text{TiO}_2@20\%\text{Fe}_2\text{O}_3$.

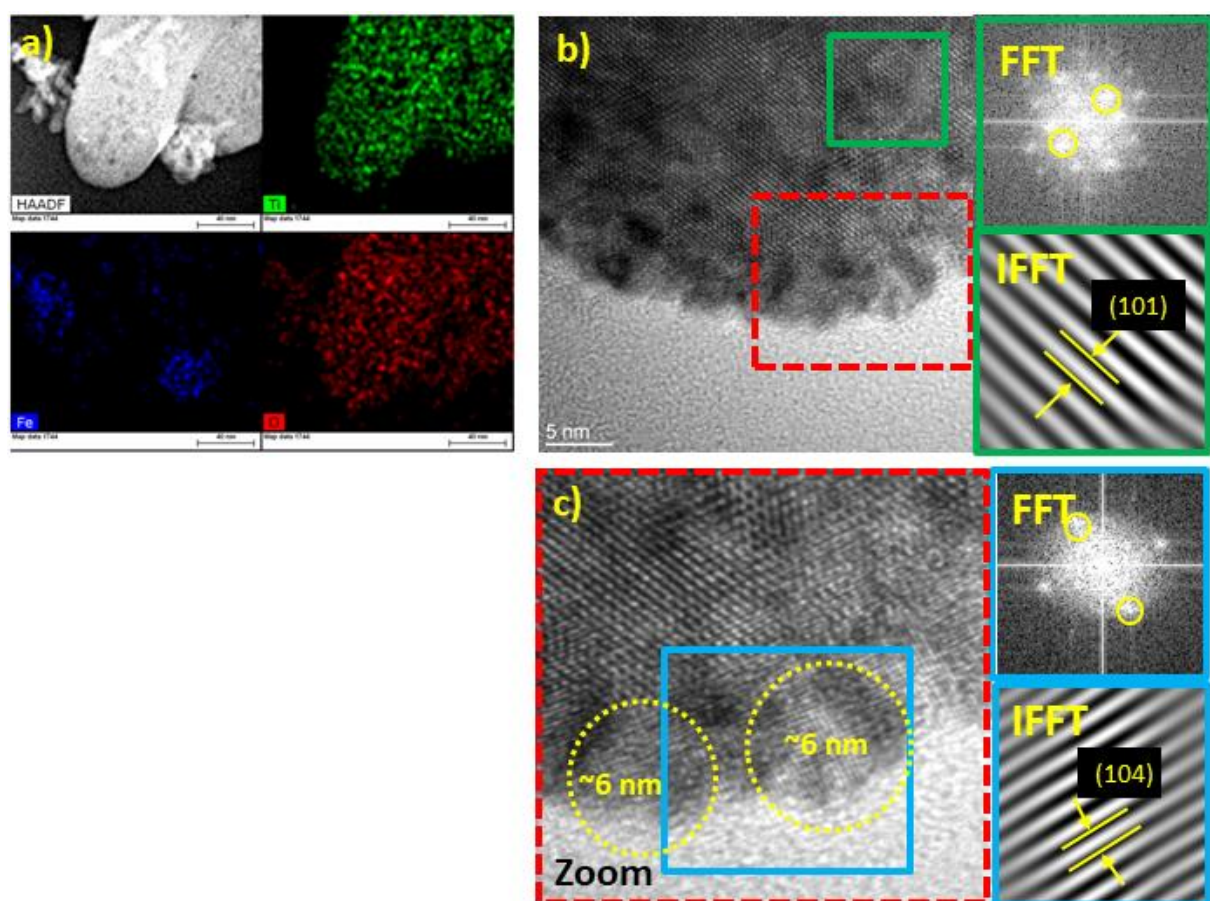


Figure S3. $\text{TiO}_2@20\%\text{Fe}_2\text{O}_3$ sample a) EDX mapping images; b) HRTEM images with Fast Fourier Transform and IFFT analysis indicate the existence of (101) plane of anatase TiO_2 ; c) FFT of the blue rectangle from the zoomed area shows hematite nanoparticles of 6 nm size with the (104) plane of $\alpha\text{-Fe}_2\text{O}_3$.

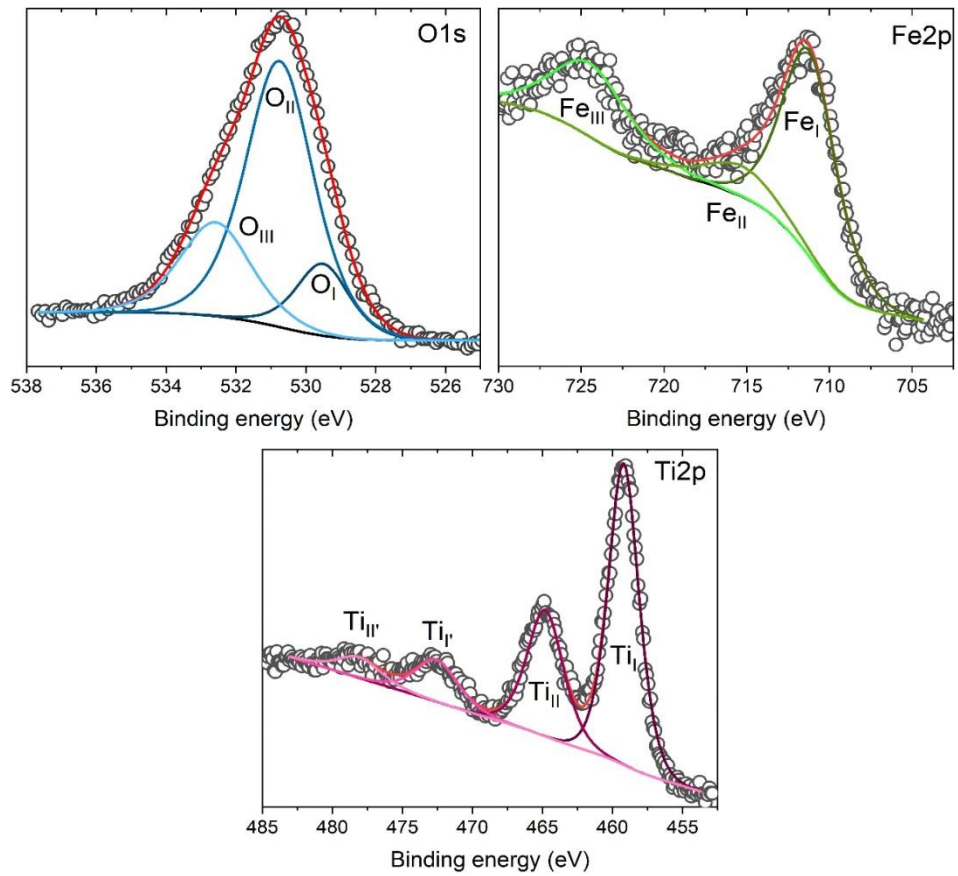


Figure S4. Deconvolution of the XPS spectra of O1s, Ti2p and Fe2p of TiO_2 nanocrystals heavily modified with Fe_2O_3 ($\text{TiO}_2@20\%\text{Fe}_2\text{O}_3$).

Table S1. Characteristic binding energies of Ti2p, O1s, and Fe2p determined from XPS analysis for TiO_2 heavily modified with Fe_2O_3 ($\text{TiO}_2@20\%\text{Fe}_2\text{O}_3$).

| Symbol | Binding energy (eV) | Type of bonding | Ref. |
|-------------|---------------------|---|-------|
| Ti2p | | | |
| TiI | 459.2(3) | $\text{Ti}2\text{p}_{3/2}$, O-Ti-O | [1] |
| TiII | 464.9(3) | $\text{Ti}2\text{p}_{1/2}$, O-Ti-O | [1] |
| TiI' | 472.7(3) | satellite of $\text{Ti}2\text{p}_{3/2}$, O-Ti-O | [1] |
| TiI'' | 478.3(3) | satellite of $\text{Ti}2\text{p}_{1/2}$, O-Ti-O | [1] |
| O1s | | | |
| OI | 529.5(4) | Ti-O-Ti | [2] |
| OII | 530.8(4) | oxygen vacancies or defects | [2] |
| OIII | 532.8(4) | chemisorbed species e.g. OH^- , H_2O , O^{2-} | [2] |
| Fe2p | | | |
| FeI | 711.5(5) | $\text{Fe}2\text{p}_{3/2}$, Fe^{3+} in Fe_2O_3 | [3-5] |
| FeII | 715.6(5) | satellite of $\text{Fe}2\text{p}_{3/2}$, Fe^{3+} in Fe_2O_3 | [3-5] |
| FeIII | 724.8(5) | $\text{Fe}2\text{p}_{1/2}$, Fe^{3+} in Fe_2O_3 | [3-5] |

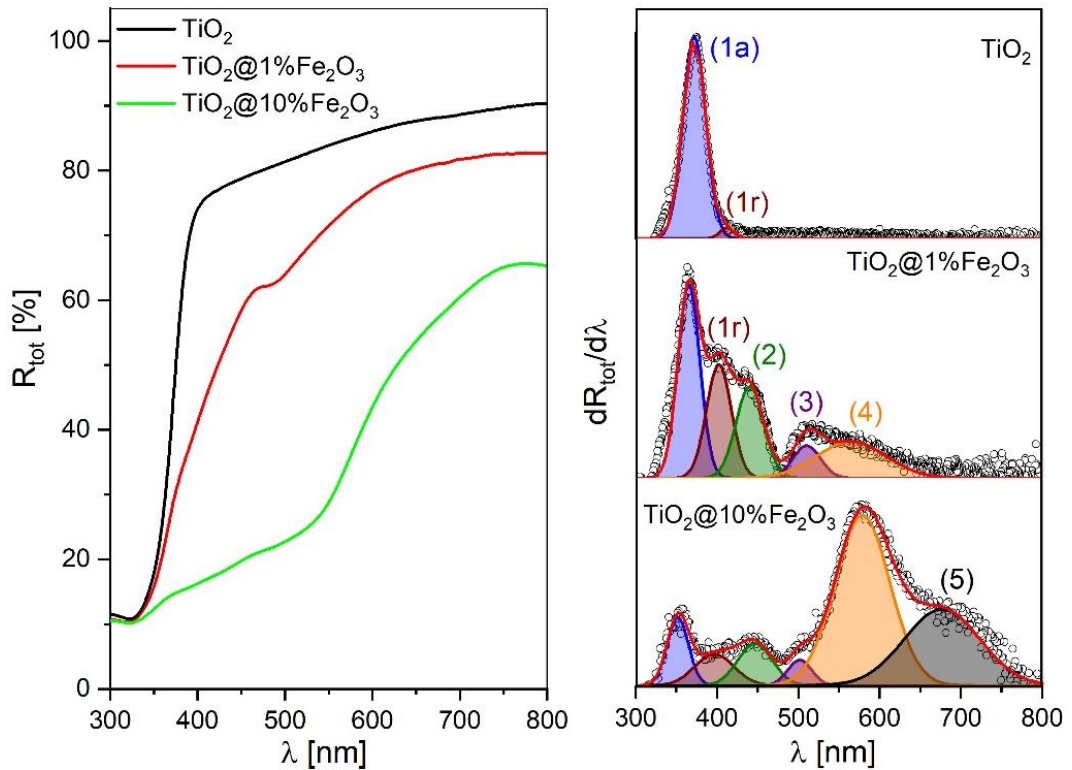


Figure S5. Spectral dependence of total reflectance (left-hand side) and first derivative spectra $dR_{\text{tot}}/d\lambda$ (right-hand side) for TiO_2 NCs before and after modification with Fe_2O_3 .

Table S2. Energies of the optical transitions for TiO_2 and $\text{TiO}_2@\text{Fe}_2\text{O}_3$ nanomaterials obtained from the first derivative plot. Transition energies were determined with an uncertainty of 0.02 eV.

| Sample | (1a) (eV) | 1r (eV) | (2) (eV) | (3) (eV) | (4) (eV) | (5) (eV) |
|--|-----------|---------|----------|----------|----------|----------|
| (TiO_2)* | 3.32 | - | - | - | - | - |
| TiO_2 | 3.34 | 3.04 | | | | |
| ($\text{TiO}_2@0.2\%\text{Fe}_2\text{O}_3$)* | 3.36 | - | 3.02 | - | - | - |
| $\text{TiO}_2@1\%\text{Fe}_2\text{O}_3$ | 3.40 | 3.08 | 2.82 | 2.43 | 2.19 | -- |
| ($\text{TiO}_2@2\%\text{Fe}_2\text{O}_3$)* | 3.43 | - | 2.92 | 2.48 | 2.17 | 1.84 |
| $\text{TiO}_2@10\%\text{Fe}_2\text{O}_3$ | 3.54 | 3.14 | 2.79 | 2.48 | 2.15 | 1.84 |
| ($\text{TiO}_2@20\%\text{Fe}_2\text{O}_3$)* | 3.52 | - | 2.81 | 2.48 | 2.13 | 1.81 |
| Fe_2O_3 | - | - | - | - | 2.11 | 1.78 |

* In this case, TiO_2 nanocrystals appears only as anatase phase.

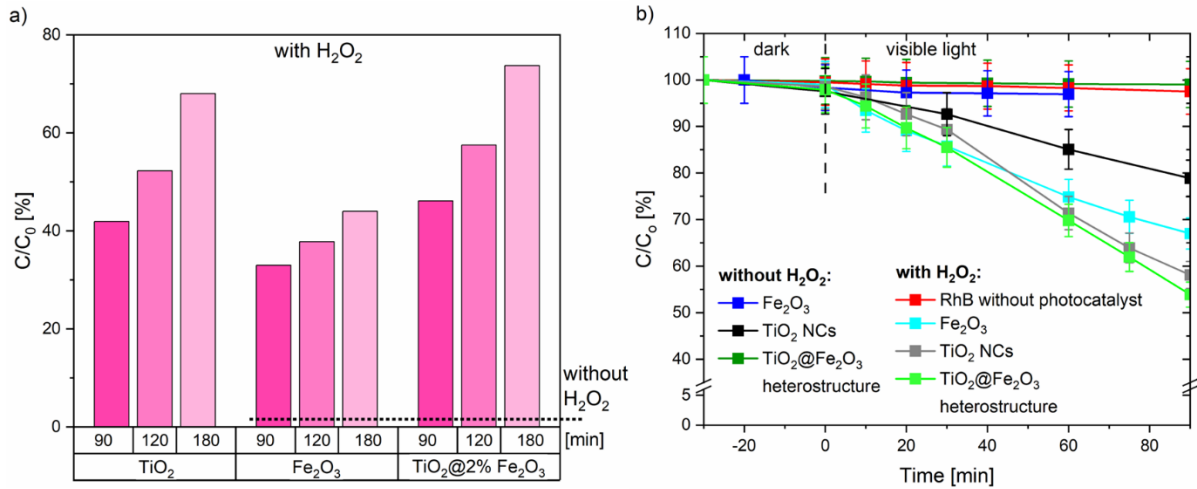


Figure S6. (a) Photocatalytic decomposition of RhB dye under visible radiation for pure oxides vs. $\text{TiO}_2@2\% \text{Fe}_2\text{O}_3$ heterojunction, (b) comparison of photocatalytic activity with and without addition of H_2O_2 to the photocatalytic system.

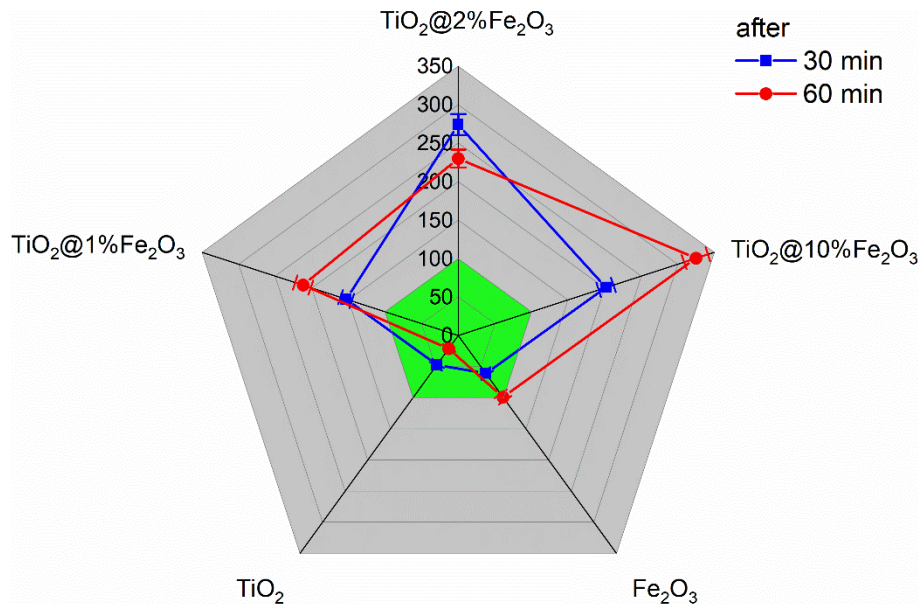


Figure S7. Normalized dye degradation after 30 and 60 min, in the presence of scavenger of holes.

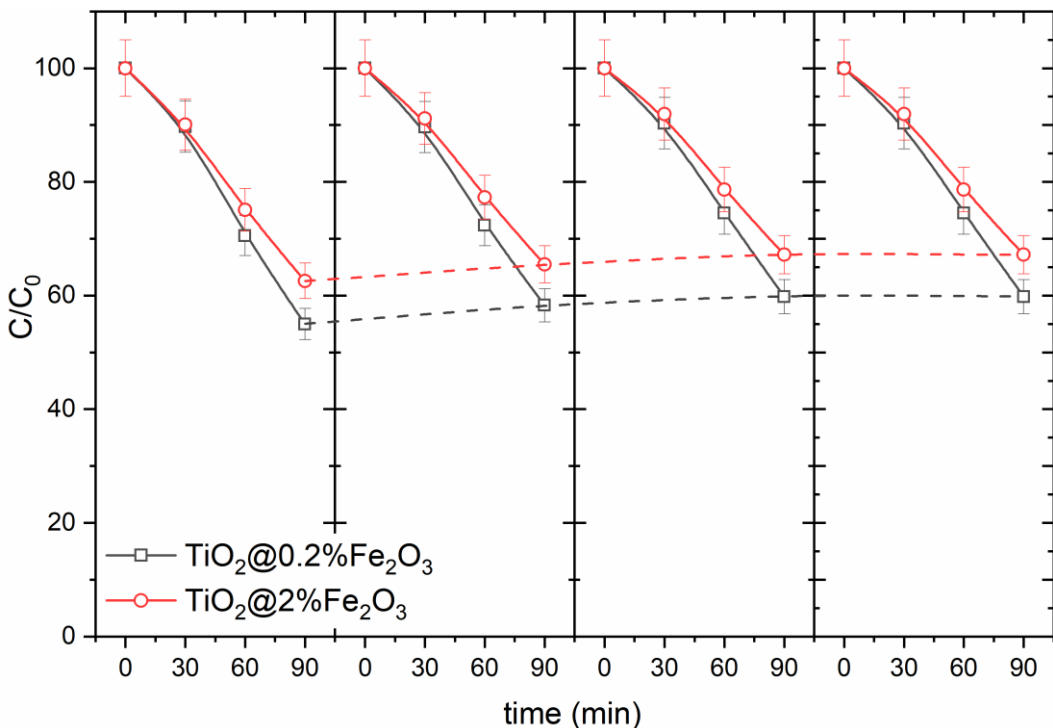


Figure S8. Recycled photocatalytic process of Rhodamine B in the presents of $\text{TiO}_2@\text{Fe}_2\text{O}_3$ and H_2O_2 .

References

1. Saha, N.C.; Tompkins, H.G. Titanium Nitride Oxidation Chemistry: An X-ray Photoelectron Spectroscopy Study. *J. Appl. Phys.* **1992**, *72*, 3072–3079, doi:10.1063/1.351465.
2. Ghobadi, A.; Ulusoy, T.G.; Garifullin, R.; Guler, M.O.; Okyay, A.K. A Heterojunction Design of Single Layer Hole Tunneling ZnO Passivation Wrapping around TiO_2 Nanowires for Superior Photocatalytic Performance. *Sci. Rep.* **2016**, *6*, 30587, doi:10.1038/srep30587.
3. Bajnóczi, É.G.; Balázs, N.; Mogyorósi, K.; Sránkó, D.F.; Pap, Z.; Ambrus, Z.; Canton, S.E.; Norén, K.; Kuzmann, E.; Vértes, A.; et al. The Influence of the Local Structure of Fe(III) on the Photocatalytic Activity of Doped TiO_2 Photocatalysts—An EXAFS, XPS and Mössbauer Spectroscopic Study. *Appl. Catal. B Environ.* **2011**, *103*, 232–239, doi:10.1016/j.apcatb.2011.01.033.
4. Yamashita, T.; Hayes, P. Analysis of XPS Spectra of Fe^{2+} and Fe^{3+} Ions in Oxide Materials. *Appl. Surf. Sci.* **2008**, *254*, 2441–2449, doi:10.1016/j.apsusc.2007.09.063.
5. Moradi, V.; Jun, M.B.G.; Blackburn, A.; Herring, R.A. Significant Improvement in Visible Light Photocatalytic Activity of Fe Doped TiO_2 Using an Acid Treatment Process. *Appl. Surf. Sci.* **2018**, *427*, 791–799, doi:10.1016/j.apsusc.2017.09.017.